High Temperatures – High Pressures, 2003/2004, volume 35/36, pages 179 – 192

DOI:10.1068/htjr089

Effective thermal conductivity of silica sand as a filling material for crevices around radioactive-waste canisters

Hiroshi Kiyohashi
Department of Mechanical Engineering, Sendai Digital Technical College, 1-4-16 Shintera, Wakabayashi-ku, Sendai 984-0051, Japan

Seizi Sasaki
Department of Mechanical Engineering, Ichinoseki National College of Technology, Hagisho-Aza-Takanashi, Ichinoseki 021-8511, Japan

Hidetoshi Masuda
Faculty of Technology, Tohoku Gakuin University, 1-13-1 Chuo, Tagajyo 985-8537, Japan
Presented at the 16th European Conference on Thermophysical Properties, Imperial College, London, England, 1 – 4 September 2002

Abstract. A method for measuring the effective thermal conductivity, λ_e, of free-falling silica sand bed is described. The sand, made artificially from quartzite, was allowed to fall into cylindrical vessels 110 mm in diameter and 120 mm high. Commercial grain size number of the sand ranged from 2 to 8 (corresponding peak diameters of the sand grains were 1680 to 74 μm). Bulk density of the sand, ρ_B, was 1180 – 1460 kg m^{-3}, and its porosity, ϕ, was 45% – 55%. λ_e was measured at the temperatures of 25, 45, 65, and 85 °C, in that order, under dry conditions, by the transient heat probe method. The measured values were found to vary with grain size number, porosity, and temperature from 0.17 to 0.46 W m^{-1} K^{-1}. The experimental results were analysed to evaluate λ_e of the sand bed in situ by means of a three-phase model previously presented.

1 Introduction

The Japanese concept for the storage of high-level radioactive waste (HLRW) assumes that stainless steel canisters containing the HLRW buried deeply underground will be surrounded by highly compact bentonite clay. In the repository, the dense clay acts as a buffer material to separate the canisters from the rock. Therefore, the thermal properties of the clay are of great relevance to the study of thermal phenomena in the repository system (Kiyohashi and Banno 1995/1996).

On the other hand, PRNFD (1992) pointed out the possibility of appearance of crevices between the canister and the buffer material, and between the buffer material and the rock. Such crevices must be filled with a good-conductance material—solid, liquid, or fine-grain—to reduce the thermal resistance of the repository system.

Many researchers, for example Kahr and Moos (1982), Knutsson (1983), Hopkirk and Wagner (1986), Kumata et al (1987), Radhakrishna and Lau (1989), Sueoka et al (1990), Susuki et al (1992), Fujita et al (1992), and Kiyohashi and Banno (1995/1996), have measured the thermophysical properties of compact bentonite by various methods. Kiyohashi and Banno (1995/1996) derived a correlation formula expressing the effective thermal conductivity, λ_e, of moist compact bentonite by means of a three-phase model. For the rock in Japan, Sato et al (1999) collected 22 378 cases of data on thermophysical and mechanical properties of rocks at great depths from about 180 published works. Kiyohashi et al (2002) recently measured λ_e of core specimens collected from three wells with a depth of 1000 m, dug in a granitoid stratum in Japan.

We have recently conducted systematic studies on the thermophysical properties of filler materials, such as bentonite powder, grains of bentonite (less than 1.7 mm, 1.7 to 4.5 mm, and 4.5 to 10 mm in diameter), silicate sand with grain size number 6,

and mixtures of silicate sand with grain size numbers 2, 3, 4, 5, 6, 7, and 8. The outline of our results was reported by Takegahara et al (2000).

The purpose of this study was, first, to obtain experimental data on the effective thermal conductivity of silica sand beds as a function of temperature and grain size, and, second, to derive a correlation formula based on the three-phase model previously developed by Kiyohashi and Deguchi (1998) in order to apply it to the thermal design of the repository system of HLRW. To achieve the second purpose, we measured also the thermal conductivity of quartzite, the mother rock of the artificial silica sand we used.

2 Measuring method

An improved heat-probe method was used for the measurement of thermal conductivity of silica sand beds and cylindrical specimens of quartzite in this study (Carslaw and Jaeger 1956; Kiyohashi et al 1983; Kiyohashi and Banno 1995/1996). Consider a homogeneous infinite medium of thermal conductivity λ with an initial temperature θ_0, into which a long straight-line heat source is inserted. If the heat source is switched on providing a constant heat output q per unit length and unit time, a curve with a constant temperature gradient versus the logarithm of time is obtained after the initial transient period. If the temperatures at the surface of the heat source are known at times $t = t_1$ and $t = t_2$ in a part of the constant temperature gradient of the curve, λ of the medium can be calculated from the following equation (Carslaw and Jaeger 1956; Kiyohashi et al 1983):

$$\lambda = \frac{q}{4\pi} \frac{\ln(t_2/t_1)}{\theta_2 - \theta_1}, \tag{1}$$

where θ is the surface temperature of the heat source, and subscripts 1 and 2 refer to times t_1 and t_2, respectively. In practice, the linear heat source (heat probe) has a finite diameter and length, and the medium is also a finite extent. After consideration of these limitations, heat probes 2.0 mm in diameter and 80 mm in effective length were designed and were also used in this study. Details of the probes were given in our previous reports (Kiyohashi et al 1983; Kiyohashi and Banno 1995/1996).

3 Materials and specimens

The sand used for the specimens in the present study consisted of artificial grains produced from quartzite mined in Okazaki city, Aichi prefecture, Japan. Table 1 shows the mineral composition and particle size indexes as defined by the American Foundrymen's Society (AFS) and the Japanese Industrial Standard (JIS). Table 2 shows grain size distributions by mesh for sands of grain size number 2 and number 3 (San-ei Silica Co. Ltd, 1999). The 'mesh' denotes size of the material passed by a screen in terms of the number of openings between the threads of net per linear inch (25.4 mm). The true density, ρ_s, of the quartzite ore measured on three cylindrical specimens described later was 2580 – 2680 kg m^{-3} (mean value: 2630 kg m^{-3}).

Table 1. Mineral composition and particle size indexes of the silica sand used.

Grain size number	Mineral composition/%				Particle size indexes, F·N	
	SiO_2	Al_2O_3	Fe_2O_3	Ig. Loss	AFS	JIS
2	98.1	0.66	0.41	0.22	(Table 2)	(Table 2)
3	97.2	0.78	0.53	0.16	(Table 2)	(Table 2)
4	98.4	0.56	0.38	0.14	19.9	32.9
5	98.5	0.51	0.36	0.22	32.4	50.7
6	98.1	0.54	0.38	0.24	66.8	119.1
7					94.4	169.7
8	93.2	2.81	1.35	0.85	197.5	369.9

Table 2. Mesh of grain size numbers 2 and 3.

Grain size number	Mesh							
	5	6	8	10	14	20	28	36
2	2.7	16.3	53.6	23.7	3.5			
3			5.7	26.8	49.5	15.1	2.5	0.4

Particle size index, F·N, is defined as gross surface area [cm^2] per unit weight [g] of sand particles. In the case of JIS Z 2601-1993, F·N is calculated from equation (2) and each particle size coefficient for each nominal size is defined in table 3:

$$F \cdot N = \sum(W_n \times S_n) / \sum W_n , \quad (2)$$

where F·N is the particle size index, W_n is the mass [g] of passed sieve material for each sieve, and S_n is the particle size coefficient given in table 3.

Table 3. Particle size coefficients for each nominal size of standard sieve.

Nominal size/μm	S_n/cm^2 g^{-1}	Nominal size/μm	S_n/cm^2 g^{-1}	Nominal size/μm	S_n/cm^2 g^{-1}
3370	5	600	31	106	178
2360	8	425	44	75	249
1700	11	300	63	53	355
1180	16	212	89	Pan[a]	631
850	22	150	125		

[a] Pan means minute particles of minus sieve of nominal size 53 μm.

The particle size coefficients in table 3 have been derived with the following four assumptions:
(i) the sand particles are spherical, with diameter D;
(ii) the sand particles are of the same diameter for a certain nominal size in each sieve;
(iii) true density of the sand particles is constant: $\rho_s = 2650$ kg m^{-3} for each nominal size of the particles;
(iv) each particle is floating separately in air, so that the particles do not contact each other.

Table 4 shows the relation between each commercial grain size number and the corresponding grain size diameter (peak diameter) prescribed in JIS G 5901-1974.

Each sand bed specimen was made of the sand of grain size numbers 2 to 8 in cylindrical heat-resistant glass vessels (100 mm inner diameter, 120 mm high, and 800 cm^3

Table 4. The relation between each grain size number and the corresponding grain diameter prescribed in JIS.

Grain size number	Peak diameter/μm (mesh)	Particle size index, F·N, in JIS
2	1680 (10)	–
3	1190 (14)	–
4	590 (28)	32.9
5	420 (35)	50.7
6	149 (100)	119.1
7	105 (150)	169.7
8	74 (200)	369.9

effective volume) by a free-falling process from a very low height. Each specimen was dried at 105 °C for 12 h in an electric drier to release free moisture from the sand bed. After natural cooling of the specimens at room temperature under air-tight conditions, they were used for the measurement of physical properties and effective thermal conductivity. Table 5 shows the bulk density, and volumetric fractions of solid, ϕ_s, and air, ϕ_a (solid and void) of the specimens of the sand bed. Two pieces of specimen, a and b, for each grain size were used as shown in the table. The abbreviation SSB preceding the specimen number stands for silica sand bed.

Table 5. Physical properties of specimens of the silica sand bed (SSB).

Specimen number	Bulk density, ρ_b/kg m^{-3}	Volumetric fraction	
		ϕ_s	ϕ_a
SSB-2a	1445	0.55	0.45
SSB-2b	1450	0.55	0.45
SSB-3a	1440	0.55	0.45
SSB-3b	1460	0.55	0.45
SSB-4a	1370	0.52	0.48
SSB-4b	1345	0.51	0.49
SSB-5a	1365	0.52	0.48
SSB-5b	1385	0.53	0.47
SSB-6a	1335	0.51	0.49
SSB-6b	1350	0.51	0.49
SSB-7a	1280	0.49	0.51
SSB-7b	1265	0.48	0.52
SSB-8a	1215	0.46	0.54
SSB-8b	1180	0.45	0.55

4 Measuring setup and procedure

The measuring setup consisted of a water bath with a temperature controller in which were three specimen containers, three heat probes, a constant power supply, an automatic switch (on a dummy load to each heat probe), a digital data recorder, a microcomputer system, etc, as shown in figure 1. The specimen container was made of stainless steel (SUS304) and its diameter and height were 127 mm and 340 mm, respectively. For the heat probe, a triple thermopile was used to increase sensitivity from 0.024 to 0.008 K μV^{-1}. Sensing points of thermocouples 1, 2, and 3 were located 35 mm, 40 mm, and 45 mm from the end of the probe, respectively (Kiyohashi and Banno 1995/1996).

The thermal conductivities of the sand beds, cores of quartzite as their mother rock, and a reference material were measured at 25, 45, 65, and 85 °C, in that order, three times at least for each experimental condition. The constant heat input, q, in equation (1) was adjusted in the ranges 1.1 – 2.6 W m^{-1} for the sand bed specimen, 5.3 – 6.6 W m^{-1} for a cylinder of high-purity (99.99% SiO_2) fused quartz (75 mm in diameter, 150 mm in height) as the reference material, and 9.8 – 16 W m^{-1} for the three cores of quartzite, so as to obtain a temperature rise of the probe of about 4 to 7 K at the end of the measurement. Its duration was set at 20 min.

The contact between the heat probe and a hole drilled in each specimen of the sand bed was very good. However, in solid cylinders, especially in the cores of quartzite (100 mm diameter, 120 mm high) the contact was not good, because the accuracy of the holes drilled with an ultrasonic machine in the cores (diameter, 2.1 to 2.5 mm) was poor because of their hardness. This appeared to increase the uncertainty of the thermal conductivity measurement.

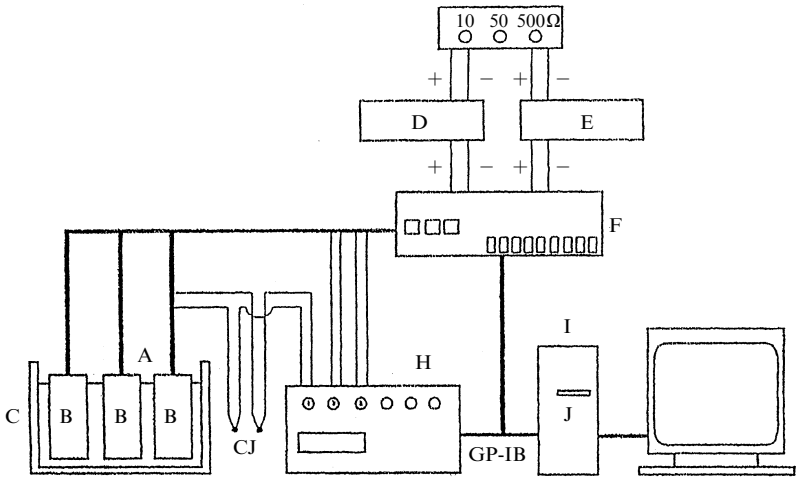

Figure 1. Setup for measuring thermal conductivity of cylindrical specimens. A, specimen container; B, specimen; C, hot water bath; D, constant power supply (1); E, constant power supply (2); F, automatic channel switch; G, dummy load; H, multi-channel digital data recorder; I, microcomputer; J, floppy drive.

5 Results and discussion

5.1 *Uncertainty of the thermal conductivity measurement*

Figure 2 shows the measured values of thermal conductivity, λ, of the cylinder of high-purity fused quartz (the reference material) versus temperature, θ. The solid line and the broken line show a regression equation and the data of Powell et al (1966), respectively. Equation (3) and R^2 are the regression equation and its coefficient of determination, respectively:

$$\lambda/\mathrm{W\ m^{-1}\ K^{-1}} = 0.0018\ \theta/^{\circ}\mathrm{C} + 1.31\,, \quad (R^2 = 0.0954)\,. \tag{3}$$

Mean values of measured λ were 1.36 W m^{-1} K^{-1} at $\theta = 30\,^{\circ}$C, and 1.45 W m^{-1} K^{-1} at $\theta = 90\,^{\circ}$C. These values are 2% below the recommended values of Powell et al (1966). However, the deviation of the measured values from equation (3) was up to $\pm 20\%$ at $\theta = 30\,^{\circ}$C and up to $\pm 5\%$ at $\theta = 90\,^{\circ}$C.

The deviation of $\pm 20\%$ at 30 °C is rather large and unsatisfactory. This defect may be due to the poor contact between the heat probe and the drilled hole. However, it seems that this has improved by thermal expansion of the heat probe at the higher temperature, $\theta = 90\,^{\circ}$C.

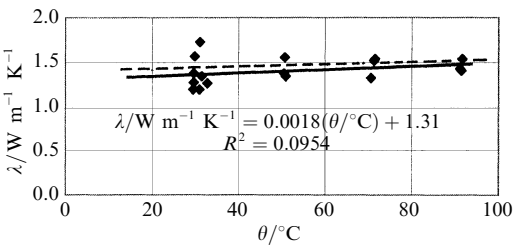

Figure 2. Thermal conductivity, λ, of high-purity fused quartz cylinder versus temperature, θ, measured with the object of testing the heat probe setup. The solid and broken lines show a regression equation and the data of Powell et al (1966), respectively.

5.2 *Experimental results for the effective thermal conductivity of SSB specimens*

Table 6 shows the results of measurements of the effective thermal conductivity, λ_e, of the silica sand bed specimens. These results indicate that the temperature dependence of λ_e is positive but very weak, and that the grain size dependence of λ_e is also positive and rather strong; that is, the value of λ_e decreases with increasing grain size number. This also means that the λ_e decreases with decreasing grain size diameter and increasing porosity, ϕ ($= \phi_a$), of the sand bed, as shown in tables 4 and 5.

Table 6. Experimental results on λ_e (W m^{-1} K^{-1}) of the SSB specimens at different temperatures (25, 45, 65, and 80 °C).

Specimen number	θ/°C				Specimen number	θ/°C			
	25	45	65	85		25	45	65	85
SSB-2a	0.291	0.253	0.288	0.322	SSB-6a	0.234	0.221	0.222	0.236
	0.291	0.389	0.331	0.347		0.234	0.242	0.221	0.262
	0.402	0.313	0.315	0.352		0.241	0.236	0.249	0.227
SSB-2b	0.317	0.319	0.311	0.342	SSB-6b	0.251	0.275	0.266	0.277
	0.412	0.311	0.327	0.362		0.281	0.257	0.262	–
	0.335	0.353	0.343	0.354		0.257	0.254	0.267	0.267
SSB-3a	0.292	0.239	0.312	0.319	SSB-7a	0.219	0.218	0.219	0.226
	0.296	0.289	0.291	0.463		0.238	0.203	0.223	0.247
	0.263	0.311	0.272	0.392		0.228	0.224	0.226	0.233
SSB-3b	0.283	0.283	0.343	0.321	SSB-7b	0.274	0.298	0.259	0.272
	0.313	0.341	0.337	0.341		0.291	0.246	0.285	0.226
	0.307	0.323	0.341	0.343		0.212	0.306	0.285	0.275
SSB-4a	0.226	0.213	0.244	0.251	SSB-8a	0.174	0.235	0.204	0.239
	0.267	0.241	0.243	0.273		0.181	0.267	0.236	0.273
	0.251	0.231	0.261	0.272		0.184	0.244	0.222	0.247
SSB-4b	0.253	0.251	0.286	0.284	SSB-8b	0.193	0.288	0.279	0.228
	0.253	0.252	0.278	0.306		0.213	0.261	0.221	0.291
	0.281	0.327	0.302	0.307		0.207	0.284	0.246	0.246
SSB-5a	0.228	0.229	0.239	0.244					
	0.272	0.263	0.263	0.276					
	0.254	0.275	0.274	0.283					
SSB-5b	0.245	0.251	0.281	0.296					
	0.309	0.293	0.292	0.314					
	0.333	0.283	0.281	0.294					

Figure 3 shows the effective thermal conductivity, λ_e, as a function of temperature, θ. In this figure, the values of λ_e are plotted against $\theta = \frac{1}{2}(\theta_1 + \theta_2)$ from equation (1). In order to obtain the correction formula between the measured values of λ_e and the specimen temperature, θ, it was assumed that λ_e could be expressed as

$$\lambda_e / \mathrm{W\ m^{-1}\ K^{-1}} = a + b(\theta/^\circ\mathrm{C})\,. \tag{4}$$

The constants a and b, and the coefficient of determination, R^2, were then obtained by linear least-squares regression, as listed in table 7.

Table 7 shows the values of coefficients a and b in equation (4), and each R^2 for all the silica sand bed specimens.

The smaller values of R^2 (which mean larger scatter of the data) for almost all of the silica sand bed specimens must be due to (i) the sand bed specimens made up from free-falling grains having a soft-structure porous body without an adhesive agent, and to (ii) unfortunately, the temperature dependence of λ_e being positive but very weak. The total values of λ_e at the 'setting temperature', θ, of 25 °C and 85 °C are 0.26 ± 0.10 W m^{-1} K^{-1}, and 0.29 ± 0.10 W m^{-1} K^{-1}.

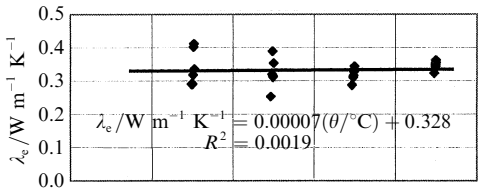

(a) SSB-2

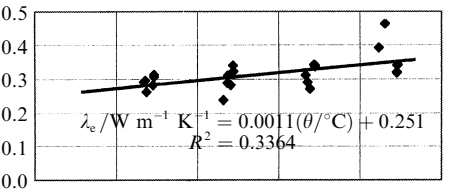

(b) SSB-3

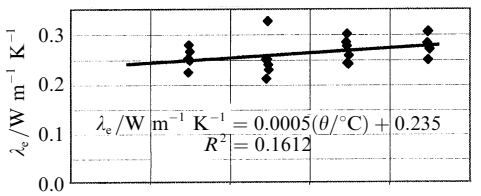

(c) SSB-4

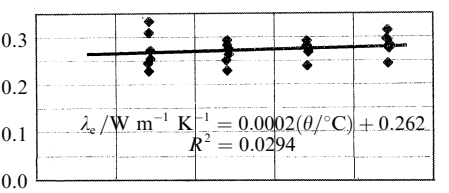

(d) SSB-5

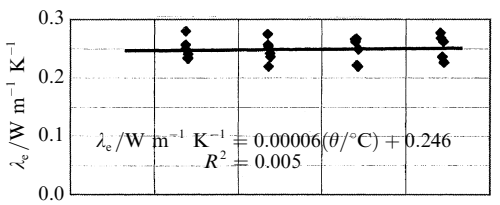

(e) SSB-6

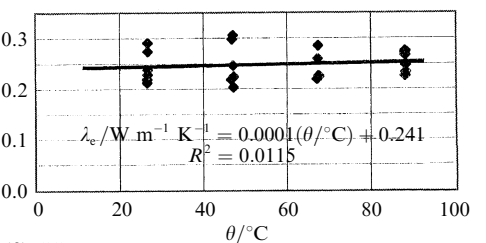

(f) SSB-7

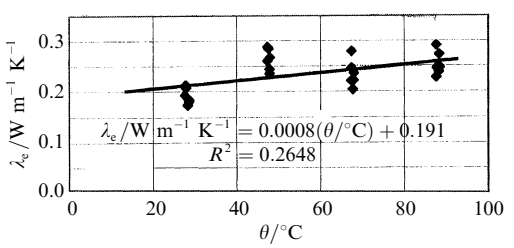

(g) SSB-8

Figure 3. Effective thermal conductivity, λ_e, of the silica sand bed specimens as a function of temperature, θ. Each solid line shows each regression line.

Table 7. Values of coefficients a and b in equation (4), and the coefficient of determination, R^2, for the silicas and specimens.

Specimen number	Coefficients		R^2
	a	b	
SSB-(2a and 2b)	0.000071	0.328	0.0019
SSB-(3a and 3b)	0.00114	0.251	0.3364
SSB-(4a and 4b)	0.000491	0.235	0.1612
SSB-(5a and 5b)	0.000199	0.262	0.0294
SSB-(6a and 6b)	0.000058	0.246	0.0049
SSB-(7a and 7b)	0.000141	0.241	0.0115
SSB-(8a and 8b)	0.000781	0.191	0.2648

Figure 4 shows λ_{ereg}, the effective thermal conductivity calculated from equation (4) for 30 °C and 80 °C as a function of particle size index, F·N. By curve fitting, the following formulae and their coefficients of determination, R^2, were obtained:

$$\lambda_{ereg} = -0.0248 \ln(\mathrm{F{\cdot}N}) + 0.3625 \quad \text{for } 30\,^{\circ}\mathrm{C},\ (R^2 = 0.8496),$$

$$\lambda_{ereg} = -0.0255 \ln(\mathrm{F{\cdot}N}) + 0.3855 \quad \text{for } 80\,^{\circ}\mathrm{C},\ (R^2 = 0.8142).$$

These high values of coefficients of determination, R^2, for the relations between λ_{ereg} and F·N show that the particle size index, F·N, could play the central role in the thermophysical phenomena in the powdered material.

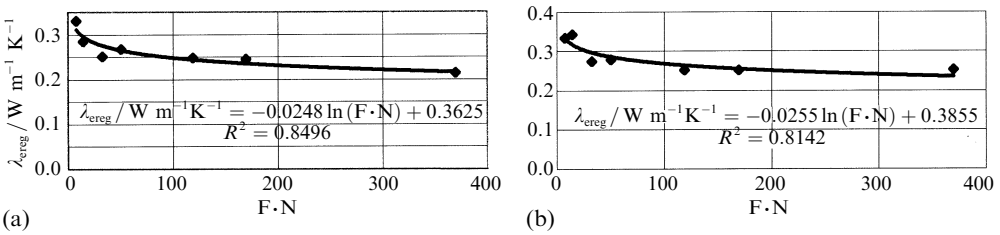

Figure 4. Regressed effective thermal conductivity, λ_{ereg}, of the silica sand bed specimens for (a) $\theta = 30\,^{\circ}\mathrm{C}$, and (b) $\theta = 80\,^{\circ}\mathrm{C}$, as a function of particle size index, F·N. Solid lines show regression equations

5.3 *Derivation of a correlation formula for λ_e based on the three-phase model*

In the underground repository system of HLRW, the free-falling silica sand beds will be compacted by gravity and some tectonic stresses after a period of time, and will absorb moisture or liquid water (Suzuki et al 1985; Bagster 1996; Eitoku et al 1997; Yu and Zou 1998). As a result, volumetric fractions of solid, liquid, and air will change, and the value of λ_e will be affected by compaction and increased moisture content, increasing with the decrease of porosity, ϕ, and the increase of volumetric fraction of water, ϕ_w. For these cases, we have tried to evaluate the values of λ_e, using the following formula (Kiyohashi and Deguchi 1998):

$$\lambda_e = \phi_s^{-k}[\lambda_s \phi_s + \lambda_w (1 - \phi_s)]^m \lambda_w^n \lambda_a^p \quad (0.05 \leqslant \phi \leqslant 0.51), \tag{5}$$

where λ_a, λ_s, and λ_w are the thermal conductivities of air, solid, and water, respectively; $p(=\phi_a)$, $m(=\phi_s)$, and $n(=\phi_w)$ are volumetric fractions of air, solid, and water, respectively; and $k = \phi_a/(\phi_a + \phi_w)$ with porosity $\phi = \phi_a + \phi_w$.

The thermal conductivities of air and water, λ_a and λ_w, can be expressed as a function of temperature with the use of the published data of Kiyohashi and Banno (1995/1996), respectively, as follows:

$$\lambda_a = 7.37 \times 10^{-5}\ (\theta/^{\circ}\mathrm{C}) + 0.0242, \tag{6}$$

$$\lambda_w = 2.36 \times 10^{-8}\ (\theta/^{\circ}\mathrm{C})^3 - 1.13 \times 10^{-5}\ (\theta/^{\circ}\mathrm{C})^2 + 2.07 \times 10^{-3}\ (\theta/^{\circ}\mathrm{C}) + 0.562. \tag{7}$$

For the silica sand bed specimen, the λ_s values can also be obtained from equation (8), by transformation of equation (5), by using the measured λ_e values, physical properties of the sand bed, and equations (6) and (7):

$$\lambda_s = \left[\left(\frac{\lambda_e}{\phi_s^{-k}\lambda_w^n \lambda_a^p}\right)^{1/m} - \lambda_w (1 - \phi_s)\right] \frac{1}{\phi_s}. \tag{8}$$

However, in the present experiment, we did not expect that λ_s will be accurate enough because of the larger scatter of the λ_e values. Therefore, we used the mother rock of the artificial silica sand to measure directly λ_s, the thermal conductivity of Aichi quartzite.

Figure 5 shows the thermal conductivity of the three cylindrical specimens made of Aichi quartzite as a function of temperature. By curve fitting, the following formula and its coefficient of determination, R^2, were obtained:

$$\lambda/\mathrm{W\ m^{-1}\ K^{-1}} = 0.0302(\theta/^{\circ}\mathrm{C}) + 4.64\,,\ (R^2 = 0.1926)\,. \tag{9}$$

This expression is barely valid because R^2 is 0.1926, but the order of λ agrees with literature data by Touloukian et al (1989). However, the temperature dependence of λ is different in the two cases. Touloukian et al found the average temperature dependence of λ of quartzite in the temperature range 300 – 1000 K to be negative. This may be correct, if one extrapolates from the temperature dependence of the thermal conductivity of high-purity quartz crystal (Touloukian et al 1989). In contrast with this, the temperature dependence of λ obtained by us is slightly positive in the temperature range 27 °C (300 K) – 90 °C (363 K) as shown in figure 5.

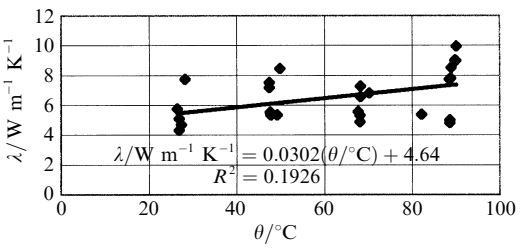

Figure 5. Thermal conductivity, λ, versus temperature, θ, in the case of cylindrical specimens of Aichi quartzite. The solid line shows a regression equation.

To check our results on λ of quartzite, we have measured it again by the following two different methods in cooperation with A Omura and T Takahashi.

Figure 6 shows the results of measurements of λ of three sets (A-1 and A-2, B-1 and B-2, and C-1 and C-2) of cubical specimens (60 mm × 60 mm × 60 mm) from the same Aichi quartzite by the hot-disk method (Omura and Tsuboi 2002). The results seem to support our results, because the dependence of λ on temperature is similar to that found by us.

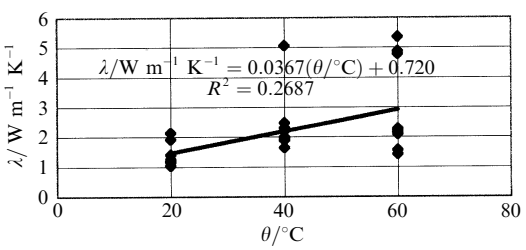

Figure 6. Thermal conductivity, λ, versus temperature, θ, for cubical specimens of Aichi quartzite reported by Omura and Tsuboi (2002). The solid line shows a regression equation.

At our request, Takahashi et al (2002) measured the thermal conductivity, λ, of the same cubical specimens of the Aichi quartzite. At prescribed three points on a diagonal line on a selected surface of each specimen, λ was measured with a thermal probe by the instantaneous-point-contact method (Takahashi and Emori 1999) at room temperature ($\theta = 27\,^{\circ}\mathrm{C}$). Table 8 shows the experimental results which express individual differences between the values of λ of specimens A, B, and C, and those measured at the three different points on the same surfaces of the specimens. Overall average of the values of λ for the eighteen different points is $\lambda_{\mathrm{Takahashi}} = 5.63 \pm 2.15\ \mathrm{W\ m^{-1}\ K^{-1}}$ at $\theta = 27\,^{\circ}\mathrm{C}$. The value of λ regressed at $\theta = 27\,^{\circ}\mathrm{C}$, obtained from equation (9) by the authors, is $\lambda_{\mathrm{Kiyohashi}} = 5.46\ \mathrm{W\ m^{-1}\ K^{-1}}$. The difference between $\lambda_{\mathrm{Takahashi}}$ and $\lambda_{\mathrm{Kiyohashi}}$ is seen to be very small.

Table 8. Experimental measurement results on λ/ W m^{-1} K^{-1} of the cubical specimens of Aichi quartzite at $\theta = 27\,^{\circ}$C by Takahashi et al (2002).

Specimen	Point 1	Point 2	Point 3	Mean
A-1	7.49	6.65	6.86	6.99 ± 0.45
A-2	6.44	7.66	6.62	6.91 ± 0.75
B-1	5.97	3.45	4.15	4.52 ± 1.45
B-2	4.56	6.05	4.89	5.17 ± 0.85
C-1	5.59	5.01	3.98	4.86 ± 0.75
C-2	5.21	5.09	5.73	5.34 ± 0.35
Overall mean				5.63 ± 2.15

For reference, the average value of λ of 140 samples of quartzite collected by Touloukian et al (1989) is 5.12 ± 2.56 W m^{-1} K^{-1} at (the estimated) room temperature and their arithmetic mean value is 5.02 W m^{-1} K^{-1}. There are very few systematic studies of the variation of thermal conductivity of quartzite with temperature between 0 and 100 °C. Ensor (1931) obtained for South African quartzite the following relation: $\lambda = -0.0102\ (\theta/^{\circ}\mathrm{C}) + 6.25$ W m^{-1} K^{-1}. The variations in the conductivity of samples of the same kind of rock 'quartzite' are much greater than would be accounted for by the uncertainties in the measurements on individual samples. These variations are undoubtedly due in part to differences in the compositions of the rock, which may have been quarried from widely separated locations.

Considering the above geological circumstance, we can regard the results by Omura and Takahashi on λ of the cubical specimens from the same Aichi quartzite as guaranteeing the quality (validity) of equation (9) obtained by us from measurements on cylindrical specimens of Aichi quartzite. However, we think that more careful measurements of λ are needed over a wider temperature range to resolve the problem of the temperature dependence and data scatter of λ.

5.4 *Evaluation of the effective thermal conductivity of silica sand bed in situ*

Evaluation of effective thermal conductivity of packing materials in situ is very important in order to establish a firm scientific basis for the safe disposal of HLRW in deep geological formations.

Kiyohashi and Deguchi (1998) proposed a three-phase correlation formula, equation (5), for the effective thermal conductivity, λ_e, of porous materials, which was derived from experimental results for 18 kinds of porous rocks under dry, moist, or water-saturated conditions.

We tried to evaluate the effective thermal conductivity of free-falling silica sand beds using equations (5), (6), (7), and (9), on the basis of the following assumptions:

(i) λ_s in equation (5) corresponds to the thermal conductivity of Aichi quartzite, expressed by equation (9);

(ii) though equation (5) was derived for rock specimens with relatively large porosities ($0.05 \leqslant \phi \leqslant 0.51$), it may also apply to specimens with much larger porosities ($0.45 \leqslant \phi \leqslant 0.55$) of the powdered material;

(iii) volume fractions ϕ_a, ϕ_s, and ϕ_w ($\phi_w = 0$ in this case) are given in table 5.

Table 9 shows a comparison of the experimental results, λ_{ereg}, of the silica sand beds calculated from the regression equation (4), and λ_{eest}, estimated from the three-phase model equation (5), and also their ratio at 30 °C and 80 °C. As shown in the table, the ratio $\lambda_{eest}/\lambda_{ereg}$ ranges from 1.35 to 2.82. The ratio is much smaller for sand beds with large-sized particles and at the lower temperature.

Table 9. Comparisons of the experimental results, λ_{ereg}, of the silica sand beds from equation (4), with estimated results, λ_{eest}, calculated from equation (5) and the related values at $\theta = 30\,^{\circ}C$ and $80\,^{\circ}C$.

Specimen	$\theta = 30\,^{\circ}C$			$\theta = 80\,^{\circ}C$		
	λ_{ereg} / W m^{-1} K^{-1}	λ_{eest} / W m^{-1} K^{-1}	$\lambda_{eest}/\lambda_{ereg}$	λ_{ereg} / W m^{-1} K^{-1}	λ_{eest} / W m^{-1} K^{-1}	$\lambda_{eest}/\lambda_{ereg}$
SSB-2	0.331	0.445	1.35	0.334	0.536	1.61
SSB-3	0.285	0.445	1.56	0.342	0.536	1.57
SSB-4	0.251	0.601	2.41	0.274	0.721	2.63
SSB-5	0.268	0.622	2.32	0.278	0.749	2.69
SSB-6	0.248	0.591	2.38	0.251	0.707	2.82
SSB-7	0.245	0.541	2.21	0.252	0.645	2.56
SSB-8	0.214	0.448	2.28	0.253	0.581	2.31

Finally, in order to try to find the reason for these results, we obtained the solid-phase thermal conductivity, λ_{sest}, estimated from another three-phase model equation (8) and the related values, as shown in table 10, figure 7, and equation (10):

$$\lambda_{sest}/\mathrm{W\ m^{-1}\ K^{-1}} = 0.01(\mathrm{F{\cdot}N}) + 2.201\,,\quad (R^2 = 0.8652)\,. \tag{10}$$

λ_{sest} increases with increase of particle size index, F·N. Precision (reliability) of equation (10) is very high because $R^2 = 0.8652$. This behaviour may be explained by increased content of high-conductivity materials, Al_2O_3 ($36 \sim 46$ W m^{-1} K^{-1}) and Fe_2O_3 in the case of grain size number 8 as shown in table 1. However, generally, λ_s must be constant regardless of the value of F·N as shown in table 10 at $\lambda_{squa} = 7.07$ W m^{-1} K^{-1} being the λ value of Aichi quartzite. But the differences between λ_{squa} and λ_{sest} are large and they may be due to the effect of thermal contact resistance between sand particles of SSB specimens.

Table 10. Results of estimated solid phase thermal conductivity, λ_{sest}, calculated from equation (8) and the related values, and some related values to thermal contact resistance between sand particles of SSB specimens at $\theta = 80\,^{\circ}C$.

Specimen	λ_{sest} / W m^{-1} K^{-1}	λ_{squa} / W m^{-1} K^{-1}	$\dfrac{\lambda_{squa} - \lambda_{sest}}{\lambda_{squa}}$	JIS F·N
SSB-2	1.736	7.07	0.7545	7.8
SSB-3	1.786	7.07	0.7474	14.7
SSB-4	3.355	7.07	0.5255	32.9
SSB-5	3.099	7.07	0.5617	50.7
SSB-6	3.176	7.07	0.5508	119
SSB-7	4.136	7.07	0.415	169.7
SSB-8	5.771	7.07	0.1837	369.9

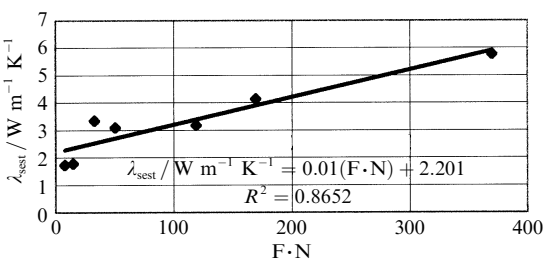

Figure 7. Estimated solid-phase thermal conductivity, λ_{sest}, calculated from equation (8) at $\theta = 80\,^{\circ}C$ versus particle size index F·N.

Solid particles of varying sizes and shapes make up the 'skeleton' of the SSB specimens. Between these solid particles are interconnected pore spaces that vary in size and shape. In perfectly dry sand, all of the pore space would be filled with air. The physical properties of the sand bed, including its ability to store water, are highly related to the fraction of the total solid volume that is occupied by the solid and the fraction that is the pore volume.

In a completely dry sand, the main mechanism of heat transmission in the sand bed is controlled by (i) heat conduction resistance within each sand particle; (ii) contact heat transfer resistance between particles; (iii) air–film thermal resistance around contact points of the particles; and (iv) conduction and radiation thermal resistance of air in the pores. Thermal resistances (ii) and (iii) will increase with an increase of F·N. However, the contribution of F·N to the total thermal resistance of the sand bed is still unknown.

Figure 8 shows the relation between $(\lambda_{squa} - \lambda_{sest})/\lambda_{squa}$ and F·N. This shows that some component of the total thermal contact resistance in the sand bed decreases with an increase of F·N.

Figure 9 shows ratios of the experimental results, λ_{ereg}, of the sand bed obtained from equation (4), and estimated results, $\lambda_{eest.FN}$ calculated from equations (5) and (10) at $\theta = 80\,^{\circ}C$ plotted against F·N. As shown in the figure, the ratio of $\lambda_{eest.FN}/\lambda_{ereg}$ is nearly equal to unity at smaller F·N, but above F·N = 32.9, the ratio increases logarithmically with increase of F·N, to 2.1 at F·N = 370.

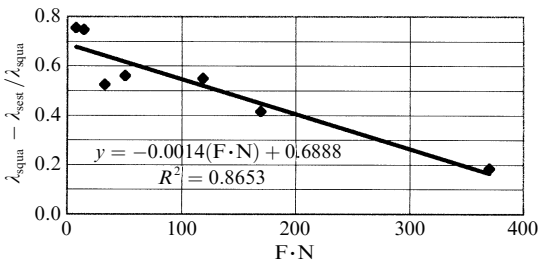

Figure 8. Relation between $y = (\lambda_{squa} - \lambda_{sest})/\lambda_{squa}$ and F·N for SSB specimens at $\theta = 80\,^{\circ}C$.

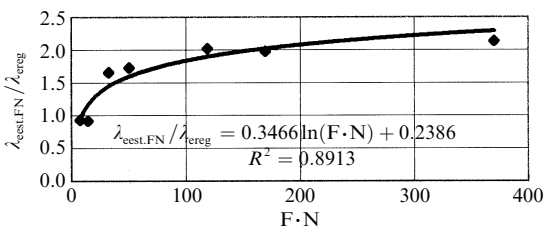

Figure 9. Ratio of effective thermal conductivities $\lambda_{eest.FN}/\lambda_{ereg}$ of SSB specimens at $\theta = 80\,^{\circ}C$ versus particle size index F·N.

The results show that we cannot apply equation (5) to estimate the effective thermal conductivity of the sand beds used in this experiment. It seems that the serious difference between λ_{sreg} and λ_{sest}, and between λ_{ereg} and $\lambda_{eest.FN}$ is mainly due to the difference in the solid structure of the two porous bodies—rocks and sand beds. The solid structure of the former is a continuum, and that of the latter is discontinuous. For this reason, if we macroscopically deal with the sand bed as one material, we must introduce, for example, a kind of apparent thermal conductivity for the solid phase of the sand beds, taking account of thermal contact resistance between the sand grains in them. Much wider application of equation (5) to macroscopically porous bodies, such as the sand bed, is a problem to be solved in the near future by more systematic experimental and model studies.

6 Conclusions

The effective thermal conductivities of fourteen macroscopic porous specimens made of free-falling artificial silica sand beds, produced in Aichi prefecture, Japan, have been measured by an unsteady heat probe method under various conditions of dry bulk density (1180 – 1460 kg m^{-3}), porosity (45% – 55%), in the temperature range of 25 to 85 °C in dry state.

Mild temperature dependence of the effective thermal conductivity was generally observed in the tested temperature range for each grain size of the sand beds. The measured effective thermal conductivity was 0.26 ± 0.10 W m^{-1} K^{-1} at 25 °C and 0.29 ± 0.10 W m^{-1} K^{-1} at 85 °C.

Particle size index, that is foundry sand number, F·N, which was defined as gross surface area per unit weight of sand particles was satisfactorily correlated with the effective thermal conductivity of all the sand bed specimens.

The experimental results were arranged and discussed in order to estimate the effective thermal conductivity of the sand bed in situ by means of a three-phase model previously presented for porous rocks. As the results of this trial ended in failure, introduction of an apparent thermal conductivity for the solid phase of the sand beds, taking account of thermal contact resistance between the sand grains, is proposed.

Acknowledgments. We would like to thank Dr I Takahashi, Yamagata University, Mr T Omura, Nichias Corporation, and their colleagues, for their academic cooperation.

References

Bagster D F, 1996 *Kona* (14) 138 – 145

Carslaw H S, Jaeger J C, 1956 *Conduction of Heat in Solids*, second edition (London: Oxford University Press) pp 261 – 262

Eitoku H, Hirota M, Suzuki M, Oshima T, 1997 *Kona* (15) 220 – 226

Ensor C R, 1931 *Proc. Phys. Soc.* **43** 581 – 591

Fujita A, Sugita H, Nouta M, Kiyohashi H, 1992, Technical Review 1410 92-052, Power Reactor and Nuclear Fuel Development Corporation, Sankaido-Biru, 1-9-B Akasaka, Minato-ku, Tokyo 107, Japan

Hopkirk R J, Wagner W H, 1986, Technical Report 85-54, Nationale Genossenschaft für die Lagerung Radioaktiver Abfälle (NAGRA), Parkstrasse 23, 5401 Baden, Switzerland

Kahr G, Müller-von Moos M, 1982, Technical Report 82-06 NAGRA, Institut für Grundbau und Bodenmechanik, ETH, Zurich, Parkstrasse 23, 5401 Baden, Switzerland

Kiyohashi H, Banno K, 1995/1996 *High Temp. – High Press.* **27/28** 653 – 663

Kiyohashi H, Deguchi M, 1998 *High Temp. – High Press.* **30** 25 – 35

Kiyohashi H, Kato H, Sato T, 2002 *High Temp. – High Press.* **34** 153 – 165

Kiyohashi H, Kyo M, Ishihama W, Tanaka S, 1983 *J. Geothermal Res. Soc. Jpn.* **5** 289 – 304

Knutsson S, 1983, Svensk Kaernbraenslefoersverining AB/Karnbranslesakerhet (SKBF/KBS) Technical Report 83-72, Sweden

Kumata M, Nakagoshi A, Shimooka K, Muraoka S, Nakamura H, 1987, Japan Atomic Energy Research Institute, Tokai-mura, Naka-gun, Ibaraki-ken 319-11, Japan, JAERI-M 87-171, pp 2 – 6

Omura T, Tsuboi M, 2002 "Measurement of thermo-physical properties of cubical specimens of Aichi quartzite by hot disk method at temperatures of 20, 40, and 60 °C", personal communication by e-mail, June 11, 2002

Powell R W, Ho C Y, Lilley P E (Eds), 1966 *Thermal Conductivity Selected Materials* volume 99, NSRDS-NBS 8 (Washington, DC: National Bureau of Standards)

PRNFD, 1992, Power Reactor and Nuclear Fuel Development Corporation report PNC TN1410 92-081(1992.9)

Radhakrishna H S, Lau K C, 1989, in *Proceedings of the Symposium: MRS Scientific Basis for Nuclear Waste Management XIII* Eds V M Oversby, P W Brown (Boston, MA: Materials Research Society) pp 725 – 732

Sato T, Taniguchi W, Fujita T, Hasegawa H, 1999, Japan Nuclear Cycle Development Institute, Technical Report JNC TN 7410

Sueoka T, Kobayashi J, Imamura S, Ogawa T, Murata S, 1990, Taisei Technical Research Report 23, Technology Research Center, Taisei Corporation, 344-1 Nasemachi, Totsuka-ku, Yokohama 245, Japan

Suzuki H, Shibata M, Yamagata J, Hirose I, Terakado K, 1992, Technical Review 8410 92-057, Power Reactor and Nuclear Fuel Development Corporation, Sankaido-Biru, 1-9-13 Akasaka, Minato-ku, Tokyo 107, Japan

Suzuki M, Ichiba H, Hasegawa I, Oshima T, 1985 *Kagaku Kogaku Ronbunshu* **11** 438 – 443

Takahashi I, Emori M, 1999 *Netsu Bussei* **13** 246 – 251

Takahashi I, Ikeno H, Koshikawa Y, 2002 "Measurements of thermo-physical properties of cubical specimens of Aichi quartzite by a thermal probe with instantaneous point contact at room temperature (1st report)", personal communication by e-mail, June 28, 2002

Takegahara T, Takao H, Sato Y, Wada H, Araoka K, Nakashima Y, Kiyohashi H, Ueda H, Kamimoto T, 2000, in Proceedings of the 55th Annual Symposium of JSCE CS-190

Touloukian Y S, Judd W R, Roy R F, 1989 *Physical Properties of Rocks and Minerals* volume II-2 of *CINDAS Data Series on Material Properties* (New York: Hemisphere) pp 473 – 477

Yu A B, Zou R P, 1998 *Kona* (16) 68 – 81